EUROPEAN ORGANIZATION FOR NUCLEAR RESEARCH

Proposal to the ISOLDE and Neutron Time-of-Flight Committee

Laser spectroscopy of neutron-rich and neutron-deficient Cadmium isotopes using MIRACLS at ISOLDE.

October 6, 2020

S. Sels[1,2], S. Malbrunot-Ettenauer[1], M.L. Bissel[1], P. Fischer[3], C. Kanitz,[1] V. Lagaki[1,3], S. Lechner[1,4], F.M. Maier[1,3], G. Neyens[1,2], W. Nörtershäuser[5], P. Plattner[1,6], L.V. Rodríguez[1], L. Schweikhard[3], M. Vilen[1], F. Wienholtz[5], D.T. Yordanov[7]

[1] *Experimental Physics Department, CERN, CH-1211 Geneva 23, Switzerland*
[2] *Instituut voor kern- en stralingsfysica, KU Leuven, Celestijnenlaan 200D, Leuven, Belgium*
[3] *Institut für Physik, Universität Greifswald, D-17487 Greifswald, Germany*
[4] *Technische Universität Wien, Karlsplatz 13, 1040 Wien, Austria*
[5] *Institut für Kernphysik, TU Darmstadt, D-64289 Darmstadt, Germany*
[6] *University of Innsbruck, A-6020, Innrain 23, Austria*
[7] *Institut de Physique Nucléaire, CNRS-IN2P3, Université Paris-Sud, 91406 Orsay, France*

Spokespersons and contact persons :
S. Sels simon.sels@cern.ch
S. Malbrunot-Ettenauer stephan.ettenauer@cern.ch

CERN-INTC-2020-068 / INTC-P-583
06/10/2020

Abstract: We propose to extend recent laser-spectroscopy work on cadmium (Cd) isotopes, performed at COLLAPS, in order to access unexplored Cd nuclides at and beyond the $N = 50$ and $N = 82$ neutron shell closures. The necessary improvement in experimental sensitivity is achieved by using MIRACLS, where ions are stored in a Multi-Reflection Time-of-Flight (MR-ToF) device while being repeatedly probed by the spectroscopy laser. In addition to spin assignments and electromagnetic moments in ^{99,131}Cd, the measurements will reveal the nuclear charge radii of ^{98,99,131,132}Cd. Fayans-based nuclear density functional theory has successfully predicted charge radii along several isotopic chains ranging from calcium all the way to cadmium and tin, thus, approaching a global description of this observable. Hence, Cd charge radii across $N = 82$ and of ^{98}Cd (^{100}Sn minus 2 protons) represent formidable benchmarks for these latest advances in nuclear theory.

Requested shifts: 22 shifts of radioactive and 4 shifts of stable beam (split into 2 runs) and 1 additional preliminary stable-beam test run.

1 Physics motivation

Nuclear charge radii are sensitive probes for a wide range of nuclear physics phenomena such as nuclear shell evolution, pairing, or deformation and shape coexistence. Hence, their accurate description all across the Segrè chart within one global theoretical framework constitutes an ambitious long-term goal of nuclear theory. In this context, nuclear density functional theory (DFT) [1] is identified as a powerful tool given its applicability over a wide range of mass numbers and nuclear observables. In recent years, significant progress has been made by modern DFT approaches to correctly reproduce nuclear charge radii. In particular, a Fayans functional Fy(Δr) has been developed which includes gradient terms in surface and pairing energies [2]. Resolving a long-standing problem for microscopic nuclear models, this functional reproduces a pronounced staggering in the charge radii between odd and even mass numbers of calcium (Ca) isotopes [3]. This behavior is observed to be especially strong between the 'doubly magic' ^{40}Ca and ^{48}Ca nuclides. Moreover, the functional's latest advancement Fy(Δr,HBF), which treats pairing correlations within the Hartree– Fock–Bogolyubov (HFB) formalism [4], performs equally well for more exotic Ca isotopes [3, 5], including the unexpectedly large charge radius of ^{52}Ca.

This same functional has been successfully employed to describe experimental nuclear charge radii of short-lived iron (Fe) [6], copper (Cu) [7], cadmium (Cd) [8], and tin (Sn) [9] isotopes, hence, a series of chemical elements with proton numbers ranging from $Z = 20$ to $Z = 50$ and involving isotopes with mass numbers from $A = 36$ to $A = 134$. This wide applicability is remarkable given that the Fayans-based DFT functional Fy(Δr,HBF) has been optimised for Ca isotopes. Fig. 1 illustrates experimental and theoretical charge radii for the isotopic chains of Cd and Sn. The Fayans functional reproduces prominent features such as the odd-even staggering, although slightly exaggerated. Furthermore, it predicts a characteristic kink which is typically found at shell closures. A sizable kink at $N = 82$ has in fact been experimentally observed in the Sn isotopes which is in ex-

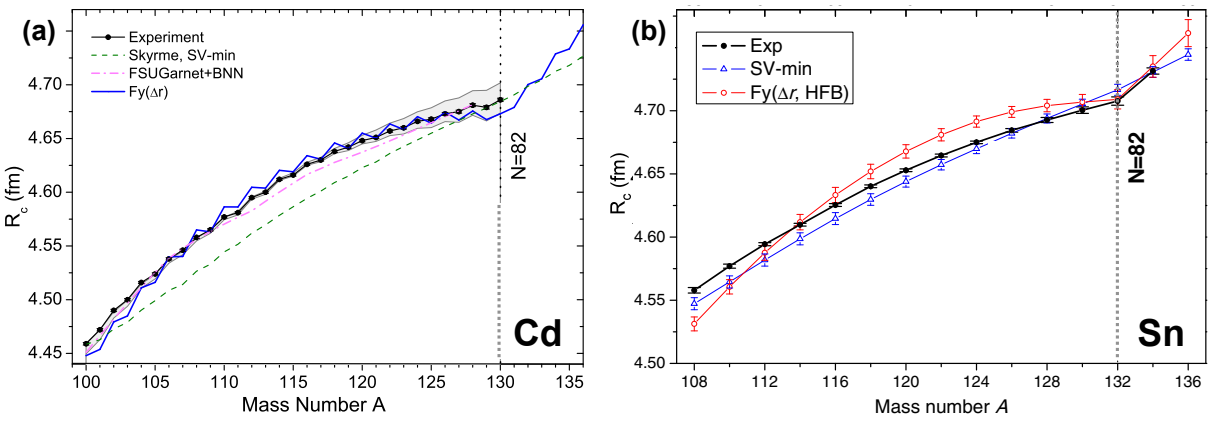

Figure 1: Rms nuclear charge radii R_c for Cd and Sn isotopes. The experimental values obtained at COLLAPS are compared to the results of density functional theory, employing the Skyrme functionals SV-min and the Fayans functional Fy(Δr). Figures from [8, 9].

cellent agreement with the Fy(Δr,HBF) calculation [9]. Note that DFT utilising Skyrme functionals such as SV-min generally fails to reproduce both; the results for the SV-min functional features neither any odd-even staggering in the Cd isotopes (see Fig. 1a) nor a kink at the shell closure $N = 82$ in the Sn isotopes (see Fig. 1b).
Fy(Δr,HBF) predicts such a kink in the Cd isotopes as well (see Fig. 1a), but previous measurements of Cd charge radii could not reach nuclides beyond $N = 82$. Investigating more neutron-rich Cd isotopes to experimentally identify the presence and magnitude of a potential kink at $N = 82$ is the primary motivation for the proposed measurements of ^{131,132}Cd. These new data will establish the signature and strength of the $N = 82$ shell-closure imprinted on the Cd charge radii on purely phenomenological grounds, in addition to a more stringent benchmark of Fy(Δr,HBF).
Despite all the recent successes of Fy(Δr,HBF), new high-quality benchmarks are in fact in demand for ongoing advancements in Fayans-based DFT. The latter are necessary to resolve remaining shortcomings in the present Fy(Δr,HBF) functional. For instance, while the Fayans functional excels in the description of the odd-even staggering and of kinks at shell closures, its general performance within a certain shell is occasionally surpassed by other DFT approaches. This can for example be seen in the Sn isotopic chain (Fig. 1b). Although a parabolic trend in the charge radii between $A = 108$ and $A = 132$ is visible for both experiment and Fy(Δr,HBF), the latter yields a much stronger curvature. Interestingly, the Skyrme functional SV-min reflects the experimental trend in the mid-shell region more closely, even though it misses the stabilising effect of the shell closure, where experimentally a relative decrease in the charge radii is observed.
Analogous conclusions also hold for the charge radii of Cu [7] and (unpublished) Ni isotopes, which motivates further improvements in Fy(Δr,HBF). A potential deficiency of the present Fayans functional could be its lack of an isovector component in the Fayans pairing functional [2, 10]. Hence, ongoing work in DFT to pin down such a (presently unused) isovector term will eventually require new experimental data to gauge the quality of this upcoming theoretical advancement. New measurements of unexplored Cd isotopes are ideally suited for this purpose given that the transition of the nuclear charge radii across the $N = 82$ shell closure has not yet been studied experimentally. Moreover, the expected relative decrease in the charge radii at the shell closure $N = 50$ defines the lower-mass end of the parabolic trend. This is precisely the region where the largest deviations between experiment and Fy(Δr,HBF) are seen for Sn. Similarly, the current Fayans-DFT results start to deflect from the experimental data for lighter Cd isotopes, see Fig. 1b. This provides the motivation for the measurement of ^{98,99}Cd in the present proposal. Note that ^{98}Cd at the neutron shell closure $N = 50$ resembles ^{100}Sn minus 2 protons and thus additionally sheds light into the structure of the presently inaccessible 'doubly magic' ^{100}Sn nucleus.
In addition to the successful DFT program on nuclear charge radii, ab-initio nuclear theory has now also reached the mass region of this proposal [11, 12]. These methods employ nuclear potentials which are linked through chiral effective field theory to the underlying forces described in quantum chromodynamics. Recent progress in ab-initio machinery allows the calculation of nuclear charge radii of the here proposed Cd isotopes. They will serve as additional benchmarks for ab-inito calculations, for instance, for ongoing work in coupled cluster theory [13] as well as in-medium similarity renormalization group [14].

Experimentally, root-mean-square (rms) nuclear charge radii can be obtained with high precision and accuracy from collinear laser spectroscopy (CLS) [15, 16, 17]. Conventional CLS has been successfully employed by COLLAPS to obtain the Cd and Sn data in Fig. 1 [8, 9]. The low production yields of the here proposed ^{98,99,131,132}Cd isotopes demand a new approach. We therefore intend to take advantage of the novel Multi Ion Reflection Apparatus for CLS (MIRACLS) for increased experimental sensitivity.

Spins and electromagnetic moments are other important nuclear observables which are directly accessible via CLS. For ^{99,131}Cd, only tentative spin assignments of $I = 5/2$ and $7/2$, respectively, are available. Nothing is experimentally known about their nuclear magnetic dipole moments μ or electric quadrupole moments Q. The study of the neutron-deficient $^{101-109}$Cd isotopes [18] suggests a simple linear trend over mass number in the electromagnetic moments for their $5/2$ ground states, similar to what has been observed in the $11/2$ states in heavier Cd isotopes [19]. Such a linear mass dependence can be explained by the unique-parity states $h_{11/2}$ and following a strict interpretation of the nuclear shell model. However, for the ground states in $^{101-109}$Cd with $I = 5/2$, an involvement of the $d_{5/2}$ orbital has to be expected. Hence, nothing prevents the unpaired neutron to migrate to neighbouring $g_{7/2}$, $s_{1/2}$, and $d_{3/2}$ orbits of identical parity. A linear trend in the electromagnetic moments as suggested by the data for these Cd isotopes is hence a priori not expected. This simplistic interpretation would predict a quadruple moment of $Q = -600$ mb for ^{99}Cd. On the other hand, a large shell model calculation results to $Q \approx -240$ mb for this nucleus [18]. Consequently, a first CLS measurement of ^{99}Cd is of importance to investigate whether a linear trend in the quadrupole moments is continued in ^{99}Cd in contrast to the shell-model calculation. More globally, as a nuclide resembling a closed-shell nucleus plus a single neutron, ^{99}Cd plays a central role in the understanding of the nuclear structure in close vicinity of ^{100}Sn. Analogously, the electromagnetic moments of ^{131}Cd, again closed-shell plus one neutron, will shed new light on the nuclear structure beyond the $N = 82$ shell closure.

2 Experimental technique

This experiment will make use of the so-called 'compact MIRACLS' setup as detailed in the INTC proposal P-565 [20]. The setup is foreseen to be located at the LA2 beamline at ISOLDE. At MIRACLS, laser spectroscopy is performed on an ion bunch that is trapped for several thousands of revolutions in a MR-ToF device. A set of photomultiplier tubes located along the center of the MR-ToF apparatus detects photons emitted by the laser-excited ions during each passing. This repeated probing of the ion bunch greatly increases the sensitivity in comparison with conventional single-pass, fluorescence-based CLS. This enables the study of more exotic isotopes with lower yields.
The MIRACLS concept has been demonstrated off-line in a proof-of-principle setup using Mg^+ ions. This element is ideal since its ionic D1 and D2 lines at ~ 280 nm represent closed 2-level systems at the fine-structure scale. Since even-mass Mg isotopes, i.e. with nuclear spin $I = 0$, exhibit no hyperfine splitting in the ionic ground state, the ions can be probed for as long as they are trapped without the need for a repump mechanism. Even-mass Cd^+ ions have a similar closed ionic system for the $^2S_{1/2} \rightarrow {}^2P_{3/2}$ transition at

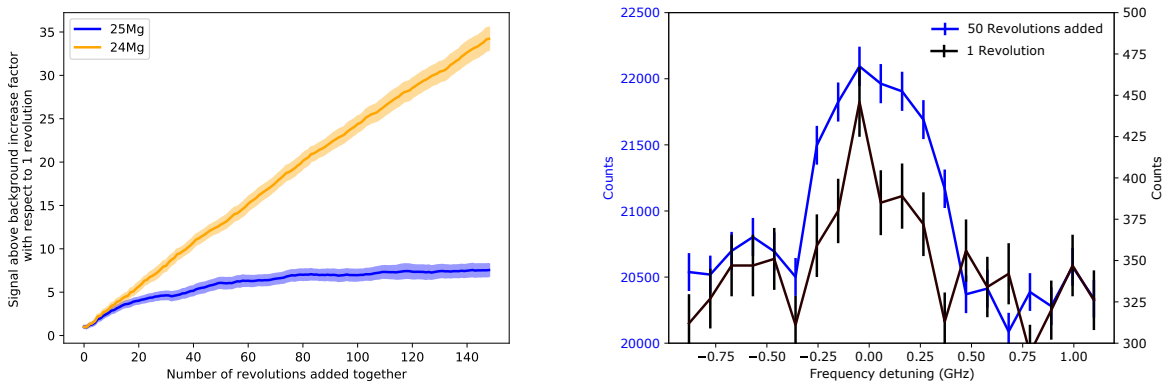

Figure 2: **(left)** Signal gain factor above background of ^{24}Mg (yellow) and ^{25}Mg (blue) versus the number of MR-ToF revolutions that is added in the data. Data from the MIRACLS PoP experiment. **(right)** Unresolved hyperfine doublet of the D1 transition line in $^{25}Mg^{+}$ ions. Comparison of the added photon signal of a single (black) versus 50 (blue) revolutions in the MIRACLS MR-ToF device with different Y-axis ranges.

215 nm. The successful operation of the proof-of-principle experiment and its similarity to Mg make Cd the ideal next science case for MIRACLS.

For closed 2-level fine-structure transitions, MIRACLS operation for nuclear spin-0 cases provides the largest signal gain over conventional CLS. However, there is a gain for odd-mass isotopes with non-zero spin as well, even though the ions are eventually pumped into other, then 'dark' hyperfine structure states. At the MIRACLS proof-of-principle setup, ^{25}Mg ($I = 5/2$) has been studied as a test case using the D1 transition line. Here, adding the signal of 50 revolutions provides a benefit over conventional CLS, which is indicated as '1 revolution' in Fig. 2. A significant improvement in signal-to-noise ratio is observed by probing the ions until they are fully pumped into the unprobed hyperfine level.

Moreover, choosing the optimal transition could allow for an even greater signal improvement for isotopes with non-zero spin. When the D2 transition line is probed in Mg^{+} ($^2S_{1/2} \rightarrow {}^2P_{3/2}$), the two hyperfine transitions labeled (34) and (21) in Fig. 3, form closed 2-level systems due to the $\Delta F \leq 1$ selection rule. I.e. this rule forces the upper F-level of these transitions to decay back into its initial ground-state level. Because of this, two out of six hyperfine peaks of $^{25}Mg^{+}$ ions could in principle benefit from an additional signal gain. In practice, a line-shape overlap to the other 4 transitions (see Fig. 3b) can partially re-open the closed 2-level system and reduces the gain in signal, especially in low-resolution CLS at MIRACLS' proof-of-principle experiment. Odd-mass Cd isotopes with $I > 1/2$ feature a transition very similar to the D2 line in $^{25}Mg^{+}$ ions. In the case of Cd^{+} ions, however, the individual 6 transitions tend to be much better resolved [18, 19]. For ^{99,131}Cd, we thus intend to take advantage of the large signal gain for the 2 closed transitions to find the position of the two hyperfine multiplets. Once located, the remaining 4 transitions can be closely probed with a signal increase comparable to what is shown in Fig. 2 for ^{25}Mg. Finally, it is being investigated whether it would be experimentally feasible to generate a second 215-nm laser beam to possibly employ a more sensitive pump-and-probe scheme for these other 4 transitions.

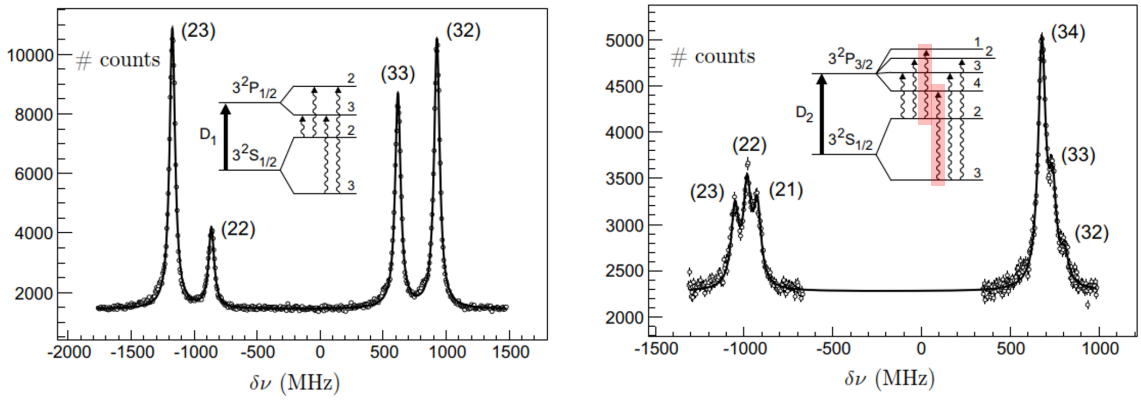

Figure 3: Hyperfine spectra for the D1 (left) and D2 (right) lines in $^{25}Mg^+$ with the respective hyperfine levels. Figure from [21]. In the D2 line, the $\Delta F \leq 1$ selection rule causes the (21) and (34) transitions shown in red to form 2 separate closed 2-level systems. Odd-mass Cd isotopes in the proposal have a one-to-one similarity to this structure.

Ions from ISOLDE will be accumulated in the ISCOOL cooler and buncher. Upon release, ion bunches will be sent to a He-filled linear Paul trap at MIRACLS. As a consequence of the tight space constraints at LA2, we opted for a compact Paul-trap design of only $\sim$ 15 cm in length. Moreover, in order to limit 're-heating' of the cooled ion bunch by ion-He collisions during the extraction and re-acceleration process, the Paul trap will be operated at low He-gas pressures. Both design choices limit the available stopping power for (heavier) incoming ions. For this reason, the ions delivered from ISCOOL will be dynamically captured by switching the voltage of the trap's upstream endcap plate when the ion bunch is fully inside the MIRACLS buncher. Simulations of ion trajectories show that a capture efficiency of around 90% can be achieved in this way at rather low pressures, while stopping a continuous beam would require pressures $> 2 \cdot 10^{-2}$ mbar for acceptable efficiency. The time of a single pass in MIRACLS' Paul trap for the present mass range is simulated to be $\sim$ 50 μs long, while the time width of ISCOOL bunches is generally around 5-10 μs. However, this capture mechanism will require testing with ^{133}Cs beam from ISCOOL, ideally prior to the ISOLDE online period. If necessary, this will allow for a potential upgrade of ISCOOL electronics to enable more narrow ion-bunch widths by a steeper voltage gradient during the ion extraction.
The laser wavelength of 215 nm will be generated by frequency quadrupling the output of a Ti-sapphire laser, pumped at 532 nm from a solid-state pump laser. This production has been successful in previous Cd experiments at COLLAPS [22, 23]. The tellurium experiment from COLLAPS that was accepted in the 64th INTC meeting will require the same laser setup for producing a 214 nm wavelength [24]. It is therefore desired to schedule these two experiments close to each other.

3 Beamtime request

We base our beam-time request on the calculated time that is necessary to reach a signal-to-noise ratio of S/N=5, assuming the most up-to-date yields [25, 12, 27], standard ef-

ficiencies in ISOLDE beam transport and results from the MIRACLS proof-of-principle setup [28, 29, 30, 31]. The extrapolation from the proof-of-principle setup is exclusively based on the number of photon detectors and the expected reduction in laser-stray light as typically achieved in an identical optical detection region at COLLAPS as described in [20]. The yields that are used in the calculation are summarized in Tab. 1.
For the neutron-deficient Cd isotopes, a clean beam is provided by a molten Sn target in combination with a plasma source. While the reported Cd yields from LaC_x and molten Sn targets are similar, optimal target operation in the latter could help in the release of the somewhat shorter-lived ^{99}Cd which could mitigate the large drop in yields from ^{100}Cd to ^{99}Cd [32]. Molten Sn targets have also been used in the past for COLLAPS and ISOLTRAP experiments on Cd isotopes [33, 34, 23, 22]. Potentially, the inclusion of an additional RILIS ionization mechanism [35, 36] could enhance the production yield in these cases [37]. We therefor favor the use of a molten Sn target.
For the neutron-rich isotopes, a UC_x target is required. Here, the presence of both cesium and barium as surface ionized, isobaric contaminants has been shown [12]. Using a tungsten neutron converter, it is possible to reduce the fraction of these contaminants. Additionally, their yield can be decreased by employing a quartz transfer line. To avoid saturation of the quartz line, we will schedule the most exotic isotope ^{132}Cd close to the start of the experimental run. Even with these methods of mitigating the isobaric contamination in place, the yield of ^{132}Cs and ^{132}Ba will be higher than ^{132}Cd [12]. As the yield of these contaminants is not expected to cause significant space-charge limitations in the MIRACLS buncher, an additional drop in count-rate for ^{132}Cd is not likely.
For the odd-mass cases, we will use the closed hyperfine transitions (see Sect 2) to locate both hyperfine triplets at first. Then, an extended scanning of these regions is necessary to measure the remaining 4 transitions. This extended laser scanning and reduced improvement factor compensates to a requested beamtime similar to some of the even-mass cases that have comparably lower yields. Our beamtime request for a division in 2 runs is as follows: A neutron-deficient run with 4 shifts for ^{98}Cd, 3.5 shifts for ^{99}Cd, 2 shifts for ^{100}Cd and systematics. A neutron-rich run with 6 shifts for ^{132}Cd, 4.5 shifts for ^{131}Cd

Table 1: Cd information and yields according to the ISOLDE yield databases [25].

Isotope	half life	Spin I^π	LaC_x Yield (ions/ μC)	UC_x Yield (ions/ μC)	Sn Yield (ions/ μC)
^{97}Cd	2.8(6) s	$(5/2)^+$	x	x	1.0×10^0
^{98}Cd	9.2(3) s	0	1.0×10^1	x	x
^{99}Cd	16(3) s	$(5/2)^+$	4.5×10^2	x	4.5×10^2
^{100}Cd	49.1(5) s	0	8.5×10^3	x	1.0×10^5
^{101}Cd	1.36(5) m	$5/2^+$	x	1.0×10^5	8.9×10^5
^{130}Cd	162(7) ms	0	x	1.0×10^4	x
^{131}Cd	68(3) ms	$(7/2)^-$	x	3×10^2 (ions/s)* [12]	x
^{132}Cd	97(10) ms	0	x	5×10^0 (ions/s)* [12]	x

$*$ Recent values at CA0 in identical target-ion-source combination as required for this proposal. These values differ from the ISOLDE database with protons directly on target [26] which results in overwhelming contamination

and 2 shifts for ^{130}Cd. Both runs would also require 2 shifts of stable beam for King plot measurements and beam tuning.
Summary of requested shifts: 22 shifts of radioactive beam time and 4 shifts of stable beam spread over 2 runs and 1 additional preliminary ISCOOL test run.

References

[1] M. Bender, et al. Self-consistent mean-field models for nuclear structure. *Rev. Mod. Phys.*, 75:121–180, Jan 2003.

[2] P.-G. Reinhard et al. Toward a global description of nuclear charge radii: Exploring the Fayans energy density functional. *Phys. Rev. C*, 95:064328, Jun 2017.

[3] R. F. Garcia Ruiz, et al. Unexpectedly large charge radii of neutron-rich calcium isotopes. *Nature Physics*, 12(6):594–598, 2016.

[4] J. Dobaczewski, et al. Mean-field description of ground-state properties of drip-line nuclei: Pairing and continuum effects. *Phys. Rev. C*, 53:2809–2840, Jun 1996.

[5] A. J. Miller, et al. Proton superfluidity and charge radii in proton-rich calcium isotopes. *Nature Physics*, 15(5):432–436, 2019.

[6] K. Minamisono, et al. Charge Radii of Neutron Deficient ^{52,53}Fe Produced by Projectile Fragmentation. *Phys. Rev. Lett.*, 117:252501, Dec 2016.

[7] R. P. de Groote, et al. Measurement and microscopic description of odd–even staggering of charge radii of exotic copper isotopes. *Nature Physics*, 2020.

[8] M. Hammen, et al. From Calcium to Cadmium: Testing the Pairing Functional through Charge Radii Measurements of $^{100-130}$Cd. *Phys. Rev. Lett.*, 121:102501, Sep 2018.

[9] C. Gorges, et al. Laser Spectroscopy of Neutron-Rich Tin Isotopes: A Discontinuity in Charge Radii across the $N = 82$ Shell Closure. *Phys. Rev. Lett.*, 122:192502, May 2019.

[10] P. G. Reinhard et al. Private Communications, 2020.

[11] T. D. Morris, et al. Structure of the Lightest Tin Isotopes. *Phys. Rev. Lett.*, 120:152503, Apr 2018.

[12] V. Manea et al. First Glimpse of the $N = 82$ Shell Closure below $Z = 50$ from Masses of Neutron-Rich Cadmium Isotopes and Isomers. *Phys. Rev. Lett.*, 124:092502, Mar 2020.

[13] G. Hagen. Private communications, 2020.

[14] J. D. Holt. Private communications, 2020.

[15] K. Blaum, et al. Precision atomic physics techniques for nuclear physics with radioactive beams. *Physica Scripta*, 2013(T152):014017, 2013.

[16] P. Campbell, et al. Laser spectroscopy for nuclear structure physics. *Progress in Particle and Nuclear Physics*, 86:127 – 180, 2016.

[17] R. Neugart *et al.* Collinear laser spectroscopy at ISOLDE: new methods and highlights. *J. Phys. G: Nucl. Part. Phys*, 44:064002, 2017.

[18] D. T. Yordanov, et al. Spins and electromagnetic moments of $^{101--109}$Cd. *Phys. Rev. C*, 98:011303, Jul 2018.

[19] D. T. Yordanov, et al. Spins, Electromagnetic Moments, and Isomers of $^{107-129}$Cd. *Phys. Rev. Lett.*, 110:192501, May 2013.

[20] M. Vilén *et al.* INTC proposal INTC-P-565. *CERN Document server*, 2020.

[21] D.T. Yordanov. *From 27Mg to 33Mg: transition to the Island of inversion.* PhD thesis, KU Leuven, 2007.

[22] M. Hammen et al. From Calcium to Cadmium: Testing the Pairing Functional through Charge Radii Measurements of $^{100-130}$Cd. *Phys. Rev. Lett.*, 121:102501, Sep 2018.

[23] D. T. Yordanov *et al.* Simple Nuclear Structure in $^{111-129}$Cd from Atomic Isomer Shifts. *Phys. Rev. Lett.*, 116:032501, Jan 2016.

[24] L. V. Rodríguez *et al.* INTC proposal INTC-P-561. *CERN Document server*, 2020.

[25] ISOLDE TISD Team. ISOLDE Yield database, 2020.

[26] U. Köster. Private communication.

[27] D. Yordanov *et al.* INTC proposal Addendum INTC-P-271-ADD-1. *CERN Document server*, 2012.

[28] F. Maier *et al.* Simulations of a proof-of-principle experiment for collinear laser spectroscopy within a multi-reflection time-of-flight device. *Hyperfine Interactions*, 240(54), May 2019.

[29] S Lechner *et al.* Fluorescence detection as a new diagnostics tool for electrostatic ion beam traps. *Hyperfine Interactions*, 240(1):95, Aug 2019.

[30] V. Lagaki *et al.* Stray-light suppression for the MIRALCS proof-of-principle experiment. *Acta Phys. Pol. B*, 51(3):571.

[31] S. Sels *et al.* First steps in the development of the Multi Ion Reflection Apparatus for Collinear Laser Spectroscopy. *Nucl. Inst. Meth B*, 463:310 – 314, 2020.

[32] T. Stora. Private communication.

[33] M. Breitenfeldt *et al.* Penning trap mass measurements of $^{99-109}$Cd with the ISOLTRAP mass spectrometer, and implications for the *rp* process. *Phys. Rev. C*, 80:035805, Sep 2009.

[34] D. T. Yordanov *et al.* Spins and electromagnetic moments of $^{101--109}$Cd. *Phys. Rev. C*, 98:011303, Jul 2018.

[35] T. Day Goodacre *et al.* Blurring the boundaries between ion sources: The application of the RILIS inside a FEBIAD type ion source at ISOLDE. *Nucl. Inst. Meth B*, 376:39 – 45, 2016.

[36] Y. Martinez Palenzuela et al. Enhancing the extraction of laser-ionized beams from an arc discharge ion source volume. *Nucl. Inst. Meth B*, 431:59 – 66, 2018.

[37] B. Marsh. Private communication.

Appendix

DESCRIPTION OF THE PROPOSED EXPERIMENT

The experimental setup comprises: MIRACLS at LA2 as described in [20].

Part of the	Availability	Design and manufacturing
MIRACLS at LA2	☒ Exisiting	☒ To be used without any modification

HAZARDS GENERATED BY THE EXPERIMENT

All hazards involving the MIRACLS installation at LA2 will be discussed with the CERN safety team as part of MIRACLS integration plan into the ISOLDE hall. Upon installation, all safety documents will be completed in close collaboration with the CERN safety team. This will be done much in advance of the first online beamtime.